#### REGULAR ARTICLE





# Tumor necrosis factor $\alpha 1$ decreases mucosal immune and antioxidant response in the midgut of hybrid fish (white crucian carp $\circ \times$ red crucian carp $\circ$ )

Ke-Xin Li<sup>1</sup> | Ning-Xia Xiong<sup>2</sup> | Jin-Fang Huang<sup>1</sup> | Shi-Yun Li<sup>1</sup> | Jie Ou<sup>1</sup> | Fei Wang<sup>1</sup> | Sheng-Wei Luo<sup>1</sup>

#### Correspondence

Sheng-Wei Luo, State Key Laboratory of Developmental Biology of Freshwater Fish, Engineering Research Center of Polyploid Fish Reproduction and Breeding of the State Education Ministry, College of Life Sciences, Hunan Normal University, Changsha 410081, Hunan, P.R. China.

Email: swluo1@163.com and swluo@hunnu.edu.cn

#### **Funding information**

National Natural Science Foundation of China, Grant/Award Number: 31902363; Hunan Provincial Natural Science Foundation of China, Grant/Award Number: 2021JJ40340

#### **Abstract**

Tumor necrosis factor  $\alpha 1$  (TNF $\alpha$ ) is a pleiotropic cytokine involved in immune regulation and cellular homeostasis, but the crucial role of TNF $\alpha$  in fish gut remained unclear. The current study aimed to evaluate the immunoregulatory function of TNF $\alpha$ 1 on gut barrier in a novel hybrid fish (WR), which was produced by crossing white crucian carp (Carassius cuvieri, Q) with red crucian carp (Carassius auratus red var,  $\eth$ ). In this study, WR- $tnf\alpha 1$  sequence was identified, and a high-level expression was detected in the intestine. Elevated levels of WR- $tnf\alpha 1$  expressions were detected in immune-related tissues and cultured fish cells on stimulation. The appearance of vacuolization and submucosal rupture was observed in TNFα1-treated midgut of WR, along with elevated levels of goblet cell atrophy, whereas no significant changes were detected in most expressions of tight-junction genes and mucin genes. In contrast, WR receiving gut perfusion with WR-TNFα1 showed a remarkable decrease in antioxidant status in midgut, whereas the expression levels of apoptotic genes and redox responsive genes increased sharply. These results suggested that TNFα1 could exhibit a detrimental effect on antioxidant defense and immune regulation in the midgut of WR.

#### KEYWORDS

crucian carp, gene expression, immune regulation, TNF $\alpha$ 1

#### 1 | INTRODUCTION

Crucian carp (*Carassius auratus*) is an important farmed fish species in China, but its farming process is affected by pathogenic infection (Lian et al., 2020). Among the documented pathogens, *Aeromonas hydrophila* is a common pathogenic bacteria that can trigger systemic infection in aquatic animals by producing virulence factors and bacterial toxins (Li et al., 2012). Hybrid fish (WR) is a novel diploid fish (2n = 100) exhibiting a strong disease resistance against pathogenic infection (Xiong et al., 2022). Our previous studies indicated that gut infection caused by *A. hydrophila* exerted a marked difference in immune and redox response in the gut–liver axis of WR, along with a

sharp increase in epithelial permeability in the midgut (Xiong, Luo, et al., 2023).

Teleost fish possess many immunoregulatory properties that can aid in host immune modulation, including pathogen recognition receptors, cytokine production, and complement cascades (Jørgensen, 2014). The reciprocal relationship among the gut, microbiota, and liver constitutes the immune microenvironment in the gut-liver axis, which has been widely studied in teleost fish (Miao et al., 2023; Xiong, Wang, et al., 2023). Mucosal layer, a biophysical barrier in the gut tract, can mediate pathogenic recognition and orchestrate the host-killing mechanism (Li et al., 2024; Salinas, 2015), but some invasive pathogens can effectively escape immune surveillance and bypass

<sup>&</sup>lt;sup>1</sup>State Key Laboratory of Developmental Biology of Freshwater Fish, Engineering Research Center of Polyploid Fish Reproduction and Breeding of the State Education Ministry, College of Life Sciences, Hunan Normal University, Changsha, P.R. China

<sup>&</sup>lt;sup>2</sup>Department of Aquatic Animal Medicine, College of Fisheries, Huazhong Agricultural University, Wuhan, P.R. China

pathogenic elimination within the host (Secombes et al., 2001). In addition, environmental stressors show a suppressive impact on fish immunity, which may render fish more vulnerable to infectious diseases (Magnadottir, 2010). Immune-regulated signals can exhibit a synergistic effect on immune regulation of gut-liver axis in fish (Wu et al., 2016). Among the known immune-related properties, tumor necrosis factor  $\alpha 1$  (TNF $\alpha$ ) is a glycopeptide hormone involved in a wide range of biological processes, which has been extensively studied in mammals (Shan et al., 2023), but teleost fish may possess multiple isoforms of  $tnf\alpha$  gene that require further research (Li et al., 2021). In addition, the immunoregulatory role of TNF $\alpha 1$  in the gut barrier of WR was unclear.

In this study, we identified and characterized  $tnf\alpha 1$  structure in WR. The expression profiles of  $tnf\alpha 1$  were measured in immunerelated tissues or cultured fish fibroblast cell (FC) lines on stimulation. Then, TNF $\alpha 1$  fusion protein was produced in vitro, and then its immunoregulatory effect on gut mucosal barrier function was studied, providing a new insight into the regulatory function of TNF $\alpha 1$  in WR.

#### 2 | MATERIALS AND METHODS

#### 2.1 | Ethical approval

All applicable international, national, and/or institutional guidelines for the care and use of animals were followed, including Chinese animal welfare laws, guidelines, and policies (GB/T 35892-2018).

#### 2.2 | Fish preparation, cell culture, and sampling

Healthy WRs were obtained from an aquaculture base in Changsha, China. Fish (c.  $19.71 \pm 1.85$  g) were acclimatized in clean fresh water ( $23.0 \pm 2.0^{\circ}$ C) and fed twice daily up to 24 h before the subsequent experiment. Then, A. hydrophila was cultured in Luria-Bertani (LB) medium at  $30^{\circ}$ C for 24 h and then resuspended in  $1\times$  phosphate-buffered saline (PBS, pH 7.3) before use. The A. hydrophila challenge group fish were intraperitoneally injected with A. hydrophila ( $1\times10^{7}$  CFU/mL), whereas the control group was administered an equivalent volume of sterile PBS. Tissues were isolated at 0, 6, 12, 24, 36, and 48 h post-injection.

WRFCs were cultured in Dulbecco's modified Eagle's medium at  $26^{\circ}$ C with a humidified atmosphere of 5% CO<sub>2</sub> as described previously (Luo et al., 2021). Then, WRFCs were seeded into six-well plates at 80% confluence for 24 h. Then, the cultured medium was replaced with a fresh medium containing 500 ng/mL of lipopolysaccharide (LPS) (*Escherichia coli* O111:B4, Sigma, USA) (Fierro-Castro et al., 2013). PBS treatment was used as the control. Cells were harvested at 0, 6, 12, 24, 36, and 48 h post-treatment. The isolated tissues and harvested cells were frozen in liquid nitrogen and preserved at  $-80^{\circ}$ C. Each group contained three biological replicates.

### 2.3 | Gene cloning, bioinformatics analysis, and plasmid construction

According to previous transcriptome data, open reading frame (ORF) sequence of WR- $tnf\alpha1$  was cloned (Xiong, Fang, et al., 2023). ORF sequence was obtained by using primers  $tnf\alpha1$ -F: ATGATGGATCTT-GAGAGTCAGCT and  $tnf\alpha1$ -R: TCATAAAGCAAACACCCCGAA. Then, the domain structure and binding sites were analysed using the EMBL-EBI database, and then the tertiary structure was produced using phyre2 programme. Moreover, the ORF sequence was ligated to pET32a and pcDNA3.1 plasmids. The constructed vectors were transformed into *E. coli*, and the positive bacterial clone was subjected to sequence confirmation (Tsingke, Beijing, China).

#### 2.4 | Dual-luciferase reporter assay

Dual-luciferase reporter assay was performed in fish cells as previously described (Yang et al., 2023). Briefly, WRFCs were seeded into 24-well plates overnight. Then, the cells were co-transfected with various amounts of recombinant vectors pcDNA3.1, pcDNA3.1-WR- $tnf\alpha$ 1, PRL-TK, and NF- $\kappa$ B Luc to investigate the transcriptional activity of NF- $\kappa$ B reporter. Furthermore, the transfected cells were stimulated with LPS at 200 ng/mL for 6 h. After 24 h, luciferase activity was analysed using a dual-luciferase reporter assay system (Promega). Relative folds of luciferase activity were normalized to the renilla luciferase level. The results were repeated in triplicate.

### 2.5 | Prokaryotic expression, purification, and validation of $TNF\alpha 1$

The fusion protein was produced and purified as described previously (Cha et al., 2015). The plasmids pET32a and pET32a-WR- $tnf\alpha1$  were transformed into *E. coli* BL21 clone, and then the positive clones were cultured in LB medium until the optical density (OD)<sub>600</sub> value reached *c.* 0.6. After a 4-h incubation with 1 mM isopropyl-beta-D-thiogalactopyranoside (IPTG), bacteria were sonicated and dissolved in urea-containing buffer. Then, supernatant proteins were purified using Ni-NTA resins. Then, the continuous protein refolding process was performed at 4°C using dialysate containing gradient-decreased urea content. Purified WR-TNF $\alpha$ 1 protein was separated using sodium dodecyl-sulfate polyacrylamide gel electrophoresis (SDS-PAGE) and validated using Western blotting. After incubation with HIS-tag primary antibody and alkaline phosphatase–conjugated secondary antibody, polyvinylidene difluoride membrane was visualized.

To validate the purified WR-TNF $\alpha 1$  fusion protein, mass spectrometry analysis was performed as described previously (Luo et al., 2020). In brief, the purified protein sample was loaded onto 12% SDS-PAGE gel, separated electrophoretically, and then subjected to peptide mass fingerprinting using a Reflex II MALDI-TOF instrument (Bruker, Germany). The information on detected peptides was

confirmed on NCBI programme (http://www.ncbi.nlm.nih.gov/blast/Blast.cgi).

#### 2.6 | Gut perfusion with TNF $\alpha$ 1

Gut perfusion assay was performed as described previously (Wang et al., 2023). Briefly, fish were anally intubated with TNF $\alpha$ 1 fusion protein (0.15 mg/per fish) by inserting a gavage needle into the hindgut, whereas an equivalent per gram of pET32 $\alpha$  tag perfusion was given to the control group. Tissues were isolated at 48 h postperfusion, immediately frozen in liquid nitrogen, and preserved at  $-80^{\circ}$ C. Each group contained three biological replicates.

#### 2.7 | Histological analysis

The isolated midgut samples were fixed in Bouin solution, dehydrated in ethanol, treated with xylene, and then embedded in paraffin wax. Then, the paraffin-embedded samples were sectioned and stained per the procedures of a periodic acid-Schiff staining kit (Jeong & Kim, 2022). Microstructures of midgut tissues were observed using a light microscope with  $200\times$  magnification. The average changes in goblet cell (GC) numbers and villus length-to-width (L/W) ratios were calculated. The experiment was repeated in triplicate.

#### 2.8 Detection of biochemical change

#### 2.8.1 | Catalase activity

Catalase (CAT) activities in the midgut were measured at  $OD_{405}$  absorbance using a CAT activity kit (Nanjing Jiancheng Bioengineering Institute, China). Results were given in units of CAT activity per milligram of protein, where 1 U of CAT is defined as the amount of enzyme decomposing 1  $\mu$ mol  $H_2O_2$  per second. The experiment was repeated in triplicate.

#### 2.8.2 | Glutathione peroxidase activity

Glutathione peroxidase (GPx) activities in the midgut were observed at  $OD_{340}$  absorbance using a GPx activity kit (Beyotime Biotechnology, China). Results were given as U/mg protein GPx activity per milligram of protein. The experiment was repeated in triplicate.

#### 2.8.3 | Total superoxide dismutase activity

Total superoxide dismutase (SOD) activity in the midgut was detected at  $OD_{560}$  absorbance using a total SOD activity kit. Results were given in units of SOD activity per milligram of protein, where 1 U of SOD is

defined as the amount of enzyme producing 50% inhibition of SOD. The experiment was repeated in triplicate.

#### 2.8.4 | Succinate dehydrogenase activity

Succinate dehydrogenase (SDH) activity in the midgut was detected at  $OD_{600}$  absorbance using an SDH activity kit. Triplicate measurements provided the mean values as U/mg protein SDH per milligram of protein.

### 2.8.5 | Determination of relative reactive oxygen species production

Reactive oxygen species (ROS) levels in supernatants of 10% midgut homogenates were measured using 2',7'-Dichlorodihydrofluorescein diacetate used for ROS detection. After triplicate repeats, ROS contents were calculated using absorbance changes at an excitation/emission wavelength of  $OD_{480/520}$  nm.

#### 2.8.6 | Malondialdehyde concentration

MDA concentration in the midgut was measured using the procedures of lipid peroxidation malondialdehyde (MDA) assay kit. The concentration of MDA was expressed as micromole MDA per milligram of protein. The experiment was repeated in triplicate.

#### 2.8.7 | Diamine oxidase activity

DAO activity in the midgut was measured using a DAO assay kit (Solarbio, China). After triplicate measurements, DAO activity was calculated using absorbance changes at  $OD_{500}$  nm.

## 2.9 | RNA isolation, complementary DNA synthesis, and quantitative reverse transcription-PCR assay

The isolated tissues and harvested cells were used for RNA isolation using the tissue total RNA isolation kit V2 (Vazyme Biotech). The isolated total RNA was treated with DNAase to avoid genomic DNA contamination. After RNA quality check, 1000 ng of purified total RNA was used to synthesize complementary DNA templates using Mon-ScriptRT III All-in-One Mix with dsNase (Monad, China). Relative expression profiles were investigated using quantitative reverse transcription-PCR (qRT-PCR) assay (Cheng et al., 2020). The primers used in this study are presented in Table S2. 18s rrna was amplified using primers RT-18s-F: CGGAGGTTCGAAGACGATCA and RT-18s-R: GAGGTTTCCCGTGTTGAGTC, which were used as internal

0958649, 0, Downloaded from https://onlinelibrary.wiley.com/doi/10.1111/jfb.15733 by Hunan Normal University, Wiley Online Library on [21/03/2024]. See the Terms and Conditions (https://onlinelibrary.wiley.com/terms

and-conditions) on Wiley Online Library for rules of use; OA articles are governed by the applicable Creative Commons License

control to normalize the results. After confirmation using melting curve analysis, qRT-PCR results were calculated using  $2^{-\triangle\triangle Ct}$  methods (Livak & Schmittgen, 2001). The calculated results were subjected to triplicate measurements.

#### 2.10 | Statistical analyses

SPSS 17 programme was used for data calculation, using one-way ANOVA or t-test analysis. Although the analytical levels reached a p-value <0.05, the results were statistically significant. The abbreviations are presented in Table S3.

#### 3 | RESULTS

### 3.1 | Characterization of $tnf\alpha 1$ nucleotide sequence and its amino acid sequence

The ORF sequence of WR- $tnf\alpha 1$  nucleotide encoded a polypeptide of 232 amino acid residues with an estimated molecular mass of 25.79 kDa and a predicted isoelectronic point of 7.21. Figure 1a shows that the secondary structure of WR-TNFα1 protein possessed 2 sheets, 2 β-hairpins, 2 β-bulges, 10 strands, and 1 disulfide. In addition, a transmembrane region, a TNF domain, seven trimer interface sites (H<sup>84</sup>F<sup>129</sup>Y<sup>131</sup>Y<sup>193</sup>F<sup>198</sup>F<sup>226</sup>F<sup>230</sup>), and six receptor binding sites  $(R^{101}K^{102}A^{107}S^{154}S^{161}S^{166})$  were observed in the structure of the WR-TNF $\alpha$ 1 protein. The multiple alignment analysis of TNF $\alpha$ 1 amino acid sequences is shown in Figure S1. Figure 1b shows that the tertiary structure of the WR-TNFα1 protein was 70% identical to c7dovB template modeled with a more than 95% confidence interval. Figure 1c shows that the tertiary structure of the WR-TNF $\alpha$ 1 protein contained 10 clefts, but only 3 clefts (marked in red, purple, and yellow) have the maximum volumes with 2949.33, 2162.11, and 2041.03 A<sup>3</sup>, respectively. Figure 1d,e shows that the structure of the WR-TNFα1 protein contained one pore with a radius of 1.22 Å and seven tunnels with the radius ranging from 1.22 to 1.50 Å.

### 3.2 | Analysis of expression profiles and transcriptional activity

Figure 2a shows that the highest expression level of WR- $tnf\alpha 1$  messenger RNA was detected in the intestine, whereas low-level expression was observed in the muscle. Figure 2b shows that WR- $tnf\alpha 1$  mRNA expression attained the peaked level at 6 h in the liver after A. hydrophila challenge. Figure 2c shows that WR- $tnf\alpha 1$  mRNA expression gradually increased from 12 to 36 h and peaked at 36 h, with the highest value in the kidney after A. hydrophila challenge. Figure 2d shows that WR receiving A. hydrophila challenge achieved the peaked expression of WR- $tnf\alpha 1$  mRNA at 12 h, but the expressions gradually declined from 24 to 48 h. Figure 2e shows that a gradual increase in WR- $tnf\alpha 1$  mRNA expression was observed in WRFCs

after a 500-ng/mL LPS exposure, and the highest expression was detected at 48 h post-stimulation.

Figure 2f shows that relative NF-κB luciferase activity increased to 10.21 and 11.82 after overexpression of 500- and 1000-ng WR- $tnf\alpha 1$  plasmid, respectively. In addition, overexpression of 500- and 1000-ng WR- $tnf\alpha 1$  plasmid could achieve a high value of 13.18 and 16.14 in NF-κB activity of WRFCs exposed to LPS stimulation.

#### 3.3 | Prokaryotic expression and validation

Figure 3 shows that a clear IPTG-induced fusion protein band was detected in pET32a-WR- $tnf\alpha1$ -transformed cells by comparing with that of pET32a-transformed cells. After Ni-NTA purification, the purified TNF $\alpha1$  fusion proteins were confirmed using Western blotting using anti-His antibody. The original Western blotting of WR-TNF $\alpha1$  fusion protein is shown in Figure S2. Then, the purified WR-TNF $\alpha1$  fusion protein was subjected to mass spectrum analysis for fusion protein validation. Table S1 presents the mass spectrum analysis of the purified fusion protein yielding four major peptides located in predicted regions, suggesting that WR-TNF $\alpha1$  fusion protein exhibited a high homology to amino acid sequences of other TNF $\alpha$ .

### 3.4 | Effect of TNF $\alpha$ 1 protein treatment on histological changes in midgut

Figure 4a,b shows that WR that received anal intubation of WR-TNF $\alpha$ 1 protein showed a remarkable increase in submucosal rupture and GC atrophy in impaired villi, along with vacuolization in the midgut. Figure 4c,d shows that the average GC numbers exhibit a 2.48-fold decrease in the villi of the WR-TNF $\alpha$ 1-perfused midgut, whereas no significant difference in L/W ratio was observed among the groups. Figure 4e shows a 3.81-fold increase in DAO activity in the midgut of WR after WR-TNF $\alpha$ 1 protein treatment. Figure 4f shows that the expression of claudin 9 and muc13 decreased remarkably in the midgut perfused with WR-TNF $\alpha$ 1 protein, whereas no significant change was observed in zo-1, occludin, claudin 1, claudin 3, claudin 6, and muc7.

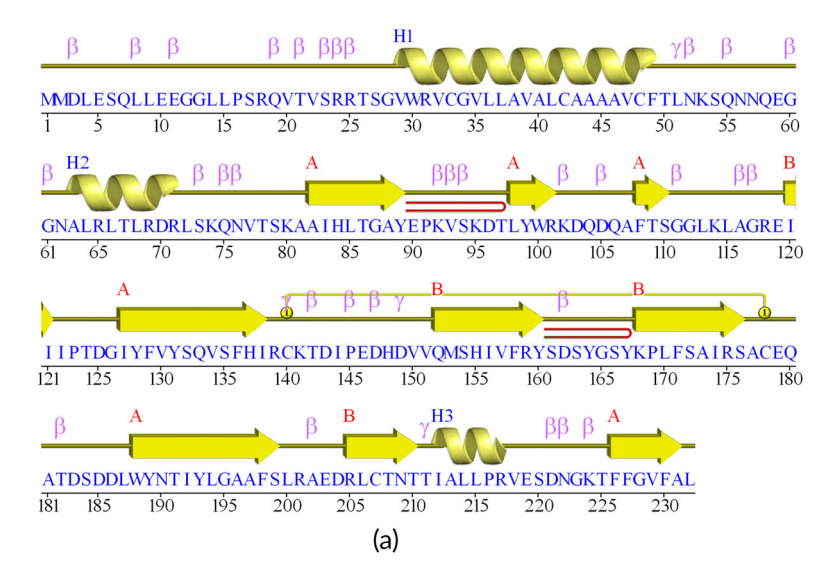
### 3.5 | Effect of TNF $\alpha$ 1 protein stimulation on immune-related gene expression in midgut

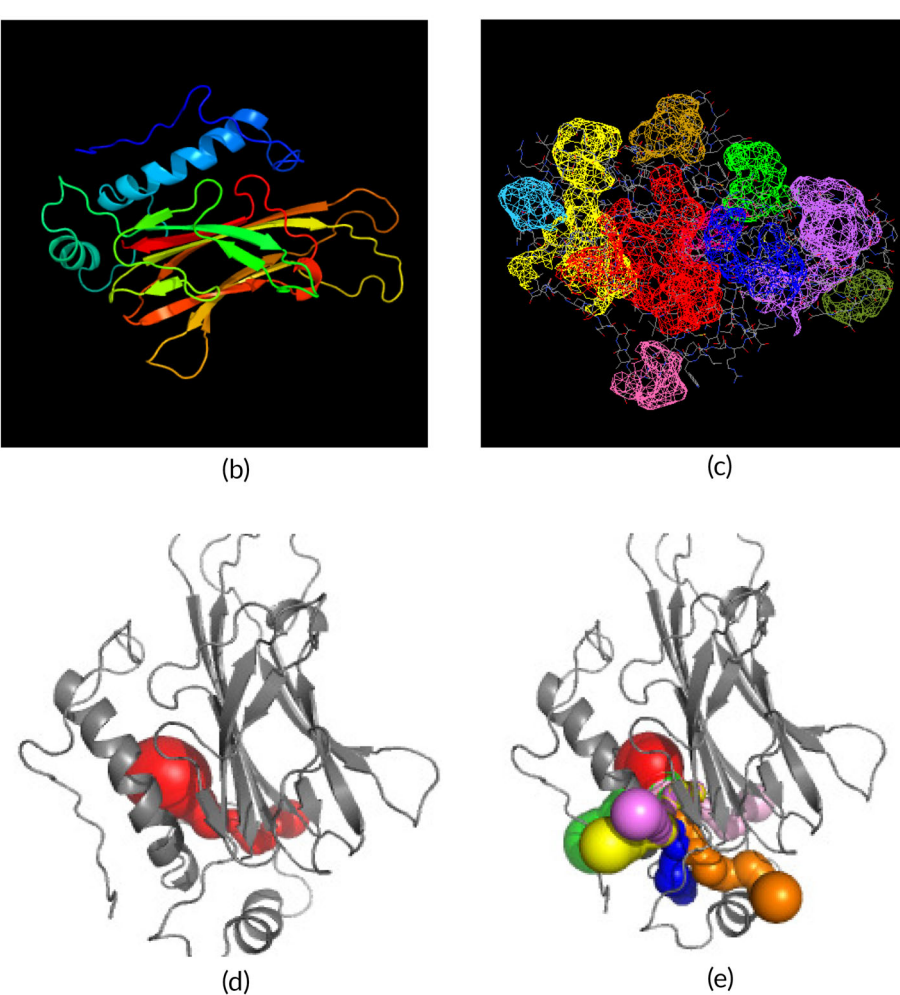
Figure 5a shows that the relative expressions of *fadd*, *casp3*, *casp7*, *casp8*, *atf4*, *atf6*, *ire1*, *pdia3*, and *xbp1* in the TNF $\alpha$ 1 protein-treated midgut were c. 2.28-, 4.37-, 4.65-, 2.12-, 2.87-, 3.11-, 2.27-, 3.78-, and 3.19-fold higher than those of the control. Figure 5b shows that the relative expressions of *hsp70*, *hsp90\alpha*, *hsp90\beta*, *oxr1*, *trxr*, and *txn1* decreased sharply in the midgut of WR after WR-TNF $\alpha$ 1 protein stimulation, whereas a 9.68- and 8.28-fold increase in *cox4* and *cyp11a1* was monitored, respectively.

10958649, 0, Downloaded from https://onlinelibrary.wiley.com/doi/10.1111/jfb.15733 by Hunan Normal University, Wiley Online Library on [21/03/2024]. See the Terms and Conditions (https://onlinelibrary.wiley.com/terms

and-conditions) on Wiley Online Library for rules of use; OA articles are governed by the applicable Creative Commons License

FIGURE 1 Bioinformatics analysis of WR-TNF $\alpha$ 1 (tumor necrosis factor  $\alpha$ 1). (a) Secondary structure prediction of WR-TNF $\alpha$ 1. - Helix strand, helices labeled: H1, H2, etc., and strands by their sheets A, B, etc.; β: βturn; γ: gamma turn; ===: β hairpin; 🚡 📆: disulfide bond. (b) Tertiary structure prediction. Structures are colored using the colors in the rainbow from N- to C-terminus. (c) Cleft domain prediction in tertiary structure of WR-TNF $\alpha$ 1. Cleft domains are colored using the colors in the rainbow. (d) Pore domain prediction. Pore domain is indicated by red. (e) Tunnel domain prediction. Tunnel domains are indicated by colors in the rainbow.





#### 3.6 | Measurement of antioxidant status in midgut

Figure 5c–e shows that fish receiving WR-TNF $\alpha$ 1 protein stimulation exhibited a 2.40-, 2.07-, 3.55-, and 2.46-fold reduction in CAT, GPx, total SOD, and SDH activities, respectively, in the midgut. In contrast, MDA concentration and ROS concentration in the WR-TNF $\alpha$ 1 protein group were, respectively, c. 3.80- and 3.42-fold higher than those of the control groups (Figure 5g,h).

#### 4 | DISCUSSION

In this study, the deduced WR-TNF $\alpha1$  polypeptide possessing the evolutionally conserved domains produced the compact jellyroll folding, which may be involved in efficient signal transduction of TNF $\alpha$ -mediated pathways (Vanamee & Faustman, 2018). In addition, increased trends in WR- $tnf\alpha1$  expressions were detected in

10958649, 0, Downloaded from https://onlinelibrary.wiley.com/doi/10.1111/jfb.15733 by Hunan Normal University, Wiley Online Library on [21.032024]. See the Terms and Conditions (https://onlinelibrary.wiley.com/terms-and-conditions) on Wiley Online Library for rules of use; OA articles are governed by the applicable Creative Commons License

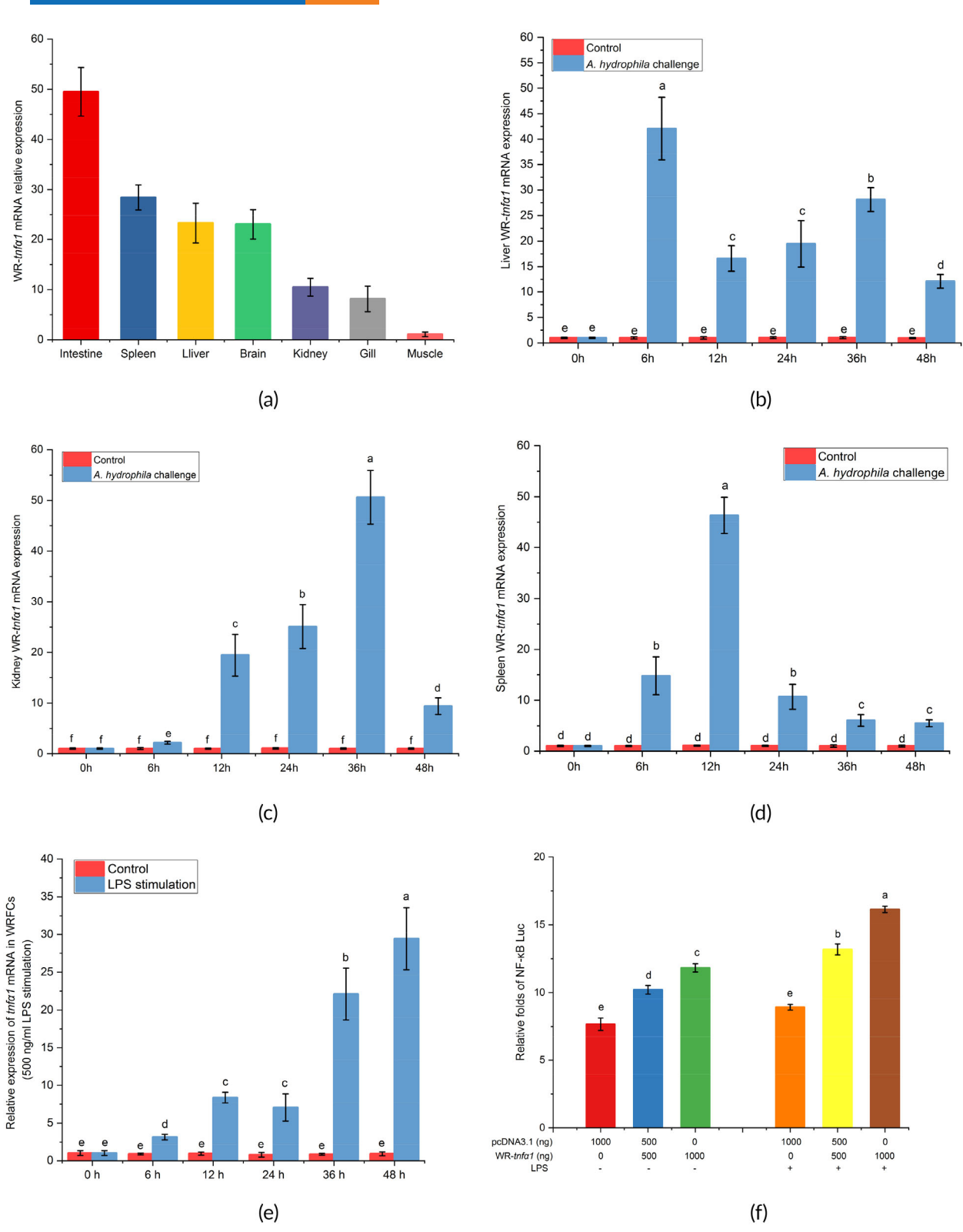


FIGURE 2 Gene expression profiles and transcriptional activity. (a) Tissue-specific expressions determined using qRT-PCR (quantitative reverse transcription-PCR) assay. 18s rrna was used as the internal control gene. (b-d) Expressions of WR- $tnf\alpha1$  were detected in the liver, kidney, and spleen at 0, 6, 12, 24, 36, and 48 h post-challenge. PBS (phosphate-buffered saline) treatment was used as the control group. 18s rrna was used as the internal control gene. (e) Expression levels of  $tnf\alpha1$  in WRFCs (WR fibroblast cell) subjected to LPS exposure. PBS treatment was used as the control group. 18s rrna was used as internal control gene. (f) Effect of WR- $tnf\alpha1$  overexpression on the promoter activities. Cells were co-transfected with PRL-TK and NF-κB Luc, together with pcDNA3.1 or pcDNA3.1-WR- $tnf\alpha1$ . The calculated data (mean ± s.d.) with different letters were significantly different (p < 0.05) among the groups. The experiments were performed in triplicate.

10958649, 0, Downloaded from https://onlinelibrary.wiley.com/doi/10.1111/jfb.15733 by Hunan Normal University, Wiley Online Library on [21/03/2024]. See the Terms

and Conditions (https://onlinelibrary.wiley.com/terms

and-conditions) on Wiley Online Library for rules of use; OA

articles are governed by the applicable Creative Commons.

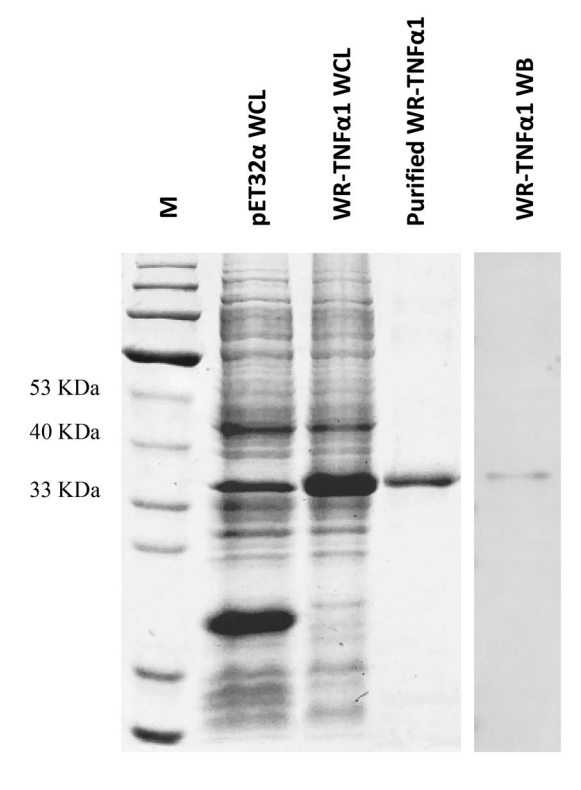


FIGURE 3 Production and validation of TNF $\alpha$ 1 fusion proteins. Lane M: protein molecular standard; lane pET32a WCL: total protein was isolated from lysis of pET32a-BL21 after IPTG induction; lane WR-TNF $\alpha$ 1 WCL: total protein was isolated from lysis of pET32a-WR-TNF $\alpha$ 1-BL21 after IPTG induction; lane-purified WR-TNF $\alpha$ 1: WR-TNF $\alpha$ 1 fusion protein was purified using Ni-NTA; lane WR-TNF $\alpha$ 1 WB: purified fusion protein was identified using anti-His tag antibody.

immune-related tissues and cultured fish cells on stimulation, implying that WR-TNF $\alpha$ 1 may be involved in fish immunity. However, the regulatory function of WR-TNF $\alpha$ 1 in gut immunity of fish is unclear.

In general, tight-junction (TJ) integrity plays an important role in immune defense against invading pathogens and functions as a physiological barrier in the gut tract (Schneeberger & Lynch, 2004). GCsecreted mucus, mucin concentrations, and bioactive molecules can facilitate immune cell communication and orchestrate mucosal immune activation (Kim & Ho, 2010; Pelaseyed et al., 2014), whereas villi deformation and DAO concentration are the predominant pathological indicators that can reflect the injured degrees of mucosal immunity in the gut tract (Zhang et al., 2020). In this study, WR receiving WR-TNF $\alpha$ 1 perfusion exhibited pathological changes in the impaired midgut, along with GC reduction and villous vacuolization. In addition, no significant changes were observed in most expression levels of TJ genes and mucin genes compared with its parental species (Huang et al., 2023; Li et al., 2024), suggesting that mucosal immune regulation of WR appeared to exhibit a higher immune tolerance against cytokine stimulation by comparing with its parental species.

The current study suggested that WR-tnfα1 overexpression could remarkably increase NF-kB activity in WRFCs with or without LPS stimulation. TNF $\alpha$ , a proinflammatory cytokine of the TNF superfamily, is able to accelerate the recruitment of downstream adaptor fas-associated with death domain protein (FADD) via TNFα receptor (Beutler & Van Huffel, 1994). FADD, a crucial component in cell death signals, can synchronize active TNF $\alpha$  signals with cysteinyl aspartate specific proteinase (CASP) molecules through the NF-kB pathway, which is involved in the choice determination between cell life and cell death events (Tourneur & Chiocchia, 2010). Death receptor-mediated extrinsic apoptosis and necroptosis are highly modulated cell death processes that can elevate immunological tolerance and remodel the inflammatory process in impaired tissues (Chen et al., 2006). In addition, TNF $\alpha$ - or oxidant-induced ROS production can exert a synergistic relationship between innate and adaptive immune response, whereas the chronic elevation of free radicals can hamper normal physiology and sabotage macromolecular bioactivity (Rizwan et al., 2014). Antioxidant enzymes and endogenous antioxidants play an important role in antioxidant response to stimuli (Sahreen et al., 2021), whereas changed activity in SDH may reflect the status of mitochondrial damage (Frederiks & Marx, 1987). Heat shock proteins (HSPs), a group of highly conserved chaperones, can function as the important stress sensors involved in protein folding, degradation, and translocation (Padmini & Usha, 2011; Yenari et al., 2005). However, continuous ROS accumulation can disrupt cellular homeostasis and hinder the redox-dependent protein folding process, which may induce increasing production of misfolded proteins in the endoplasmic reticulum (Chong et al., 2017). As is well known, unfolded protein response (UPR) is an integrated signal pathway that can attenuate the biosynthetic burden of misfolded proteins and cope with the stressors jeopardizing the normal function of all living cells (Liu & Kaufman, 2003). Activation of UPR signals can exert a cytoprotective effort on homeostasis recovery in tissues or cells suffering from detrimental stressors and severe illness, whereas its subversion may exacerbate immune and antioxidant insult (Celli & Tsolis, 2015). In this study, WR-TNFα1 perfusion could alleviate the expression profiles of antioxidant genes in the midgut of WR, whereas the expressions of apoptotic genes, UPR genes, and redox responsive genes increased sharply. In addition, antioxidant enzyme activities decreased significantly TNFα1-perfused midgut, along with increased levels of ROS production and MDA concentration. These results indicated that ROSinduced cytotoxic stress was involved in antioxidant insult and apoptotic process in TNF $\alpha$ 1-treated midgut of WR.

In conclusion, this study was the first to characterize WR-TNF $\alpha$ 1 architecture. Expression patterns of  $tnf\alpha$ 1 in tissues and fish cells were measured. WR- $tnf\alpha$ 1 overexpression could elevate NF- $\kappa$ B activity in WRFCs. Gut perfusion with WR-TNF $\alpha$ 1 could reduce GC numbers and alleviate antioxidant status in the midgut of WR, whereas apoptotic gene expressions increased sharply. Our results revealed that the toxicological effect of WR-TNF $\alpha$ 1 may cause the collapse of antioxidant capacity and promote apoptotic process in the midgut of WR.

10958649, 0, Downloaded from https://onlinelibrary.wiley.com/doi/10.1111/jfb.15733 by Hunan Normal University, Wiley Online Library on [21.032024]. See the Terms and Conditions (https://onlinelibrary.wiley.com/terms

and-conditions) on Wiley Online Library for rules of use; OA articles are governed by the applicable Creative Commons License

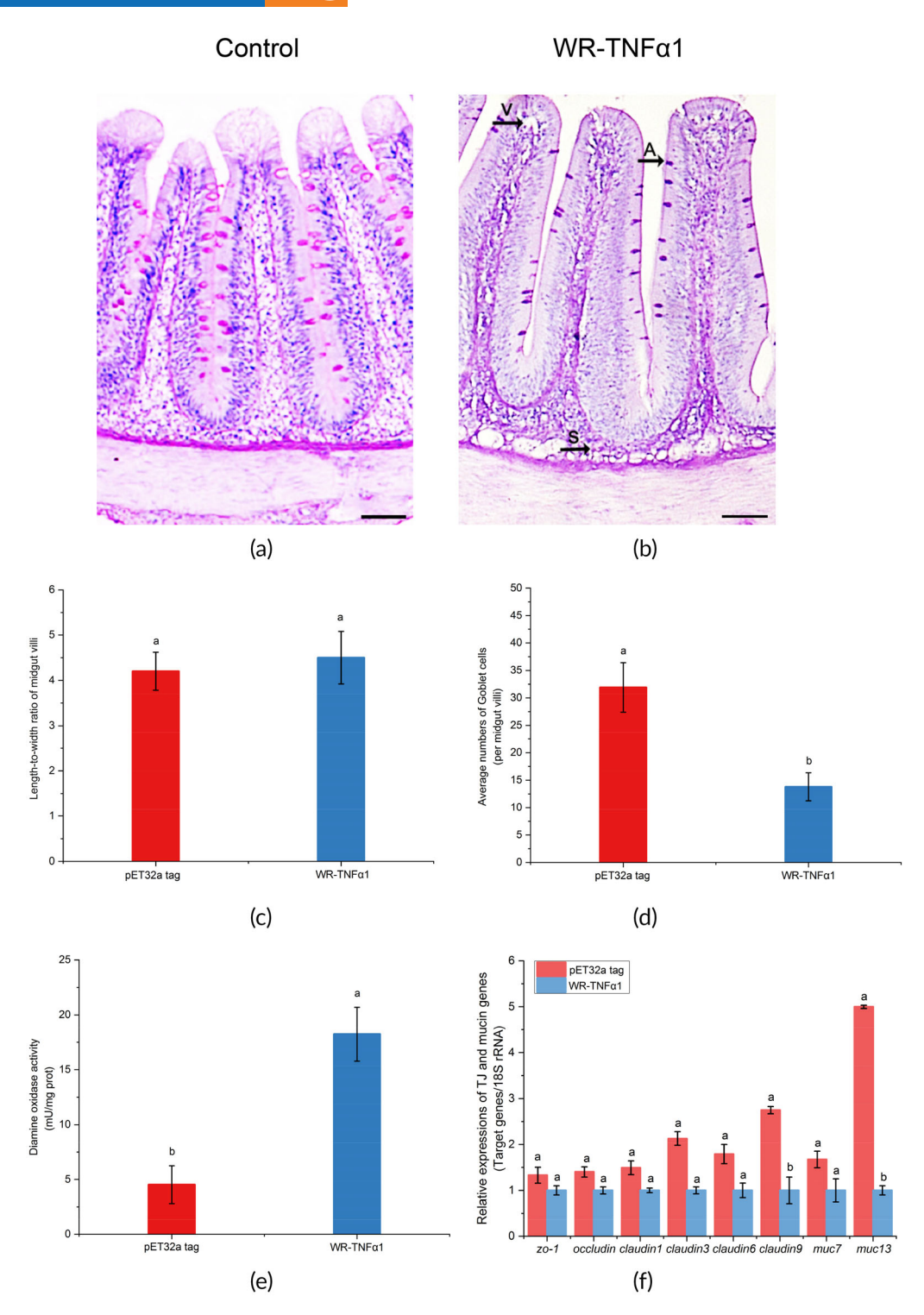
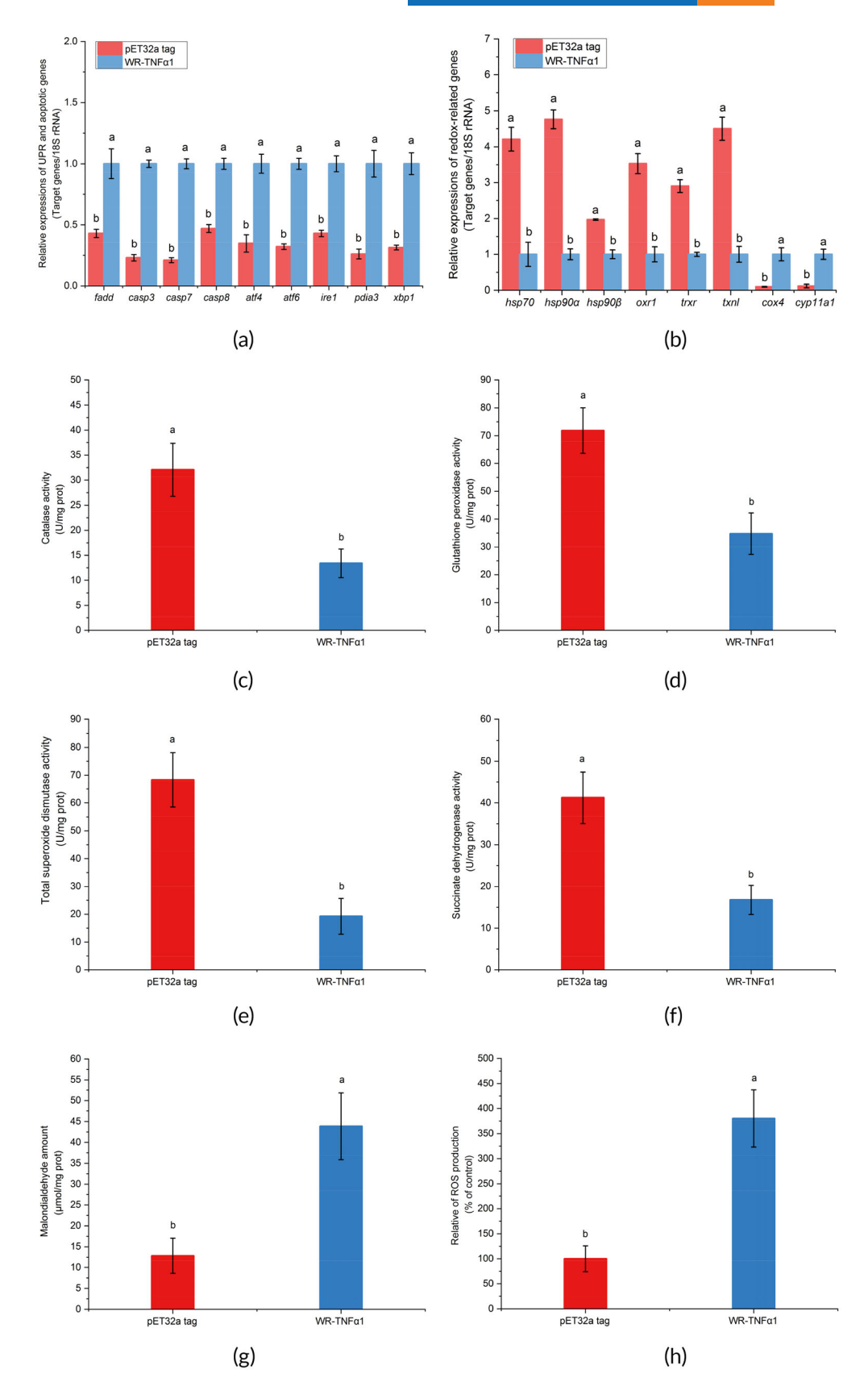


FIGURE 4 Histological analysis in midgut by in vivo administration of WR-TNF $\alpha$ 1 fusion protein. (a,b) Midgut tissues were sectioned and stained using the PAS (periodic acid-Schiff) staining kit. A: goblet cell atrophy, S: submucosal rupture, and V: villus vacuolization. (c) Villus length-to-width (L/W) ratios, (d) average numbers of goblet cells, and (e) midgut DAO (diamine oxidase) activities were determined. (f) Expressions of TJ (tight-junction) genes and mucins in midgut perfused with WR-TNF $\alpha$ 1. The calculated data (mean ± s.d.) with different letters were significantly different (p < 0.05) among the groups. The experiments were performed in triplicate.

10958649, 0, Downloaded from https://onlinelibrary.wiley.com/doi/10.1111/jfb.15733 by Hunan Normal University, Wiley Online Library on [21.032024]. See the Terms and Conditions (https://onlinelibrary.wiley.com/terms-and-conditions) on Wiley Online Library for rules of use; OA articles are governed by the applicable Creative Commons License

FIGURE 5 In vivo administration of WR-TNF $\alpha$ 1 fusion protein regulated immune response in the midgut. (a) Expressions of apoptosis genes and UPR (unfolded protein response) genes in the midgut perfused with WR-TNF $\alpha$ 1. (b) Expressions of antioxidant genes and redox responsive genes in the midgut perfused with WR-TNF $\alpha$ 1. (c-f) CAT (catalase), GPx (glutathione peroxidase), total SOD (superoxide dismutase), and SDH (succinate dehydrogenase) were detected in the midgut. (g, h) MDA (malondialdehyde) concentration and ROS (reactive oxygen species) production were determined in the midgut. The calculated data (mean ± s.d.) with different letters were significantly different (p < 0.05) among the groups. The experiments were performed in triplicate.



#### **AUTHOR CONTRIBUTIONS**

Ke-Xin Li and Ning-Xia Xiong performed methodology and formal analysis; Shi-Yun Li, Jin-Fang Huang, Jie Ou, and Fei Wang performed verification; Sheng-Wei Luo performed conceptualization, supervision, project management, and article writing.

#### **FUNDING INFORMATION**

This research was supported by the National Natural Science Foundation of China, China (grant no.: 31902363), and Hunan Provincial Natural Science Foundation of China, China (grant no.: 2021JJ40340).

#### DATA AVAILABILITY STATEMENT

The data are available from the corresponding author on reasonable request.

#### **ORCID**

Sheng-Wei Luo https://orcid.org/0009-0005-6656-5201

#### REFERENCES

- Beutler, B., & Van Huffel, C. (1994). Unraveling function in the TNF ligand and receptor families. *Science*. 264, 667–668.
- Celli, J., & Tsolis, R. M. (2015). Bacteria, the endoplasmic reticulum and the unfolded protein response: Friends or foes? *Nature Reviews Microbiology*, 13, 71–82.
- Cha, G.-H., Luo, S.-W., Qi, Z.-H., Liu, Y., & Wang, W.-N. (2015). Optimal conditions for expressing a complement component 3b functional fragment (α2-macroglobulin receptor) gene from Epinephelus coioides in Pichia pastoris. Protein Expression and Purification, 109, 23–28.
- Chen, M., Wang, Y.-H., Wang, Y., Huang, L., Sandoval, H., Liu, Y.-J., & Wang, J. (2006). Dendritic cell apoptosis in the maintenance of immune tolerance. *Science*, 311, 1160–1164.
- Cheng, C.-H., Su, Y.-L., Ma, H.-L., Deng, Y.-Q., Feng, J., Chen, X.-L., Jie, Y.-K., & Guo, Z.-X. (2020). Effect of nitrite exposure on oxidative stress, DNA damage and apoptosis in mud crab (Scylla paramamosain). *Chemosphere*, 239, 124668.
- Chong, W. C., Shastri, M. D., & Eri, R. (2017). Endoplasmic reticulum stress and oxidative stress: A vicious nexus implicated in bowel disease pathophysiology. *International Journal of Molecular Sciences*, 18, 771.
- Fierro-Castro, C., Barrioluengo, L., López-Fierro, P., Razquin, B., & Villena, A. (2013). Fish cell cultures as in vitro models of inflammatory responses elicited by immunostimulants. Expression of regulatory genes of the innate immune response. Fish & Shellfish Immunology, 35, 979–987.
- Frederiks, W. M., & Marx, F. (1987). Changes in cytoplasmic and mitochondrial enzymes in rat liver after ischemia followed by reperfusion. Experimental and Molecular Pathology, 47, 291–299.
- Huang, J.-F., Xiong, N.-X., Li, S.-Y., Li, K.-X., Ou, J., Wang, F., & Luo, S.-W. (2023). Tumor necrosis factor  $\alpha 1$  (TNF $\alpha 1$ ) administration can disrupt barrier function and attenuate redox defense in midgut of red crucian carp (Carassius auratus red var). *Reproduction and Breeding*, 3, 208–218.
- Jeong, M. K., & Kim, B.-H. (2022). Grading criteria of histopathological evaluation in BCOP assay by various staining methods. *Toxicological Research*, 38, 9–17.
- Jørgensen, J. B. (2014). The innate immune response in fish. Fish Vaccination, 1, 84–102.
- Kim, Y. S., & Ho, S. B. (2010). Intestinal goblet cells and mucins in health and disease: Recent insights and progress. *Current Gastroenterology Reports*, 12, 319–330.

- Li, M., Wang, Q.-I., Lu, Y., Chen, S.-L., Li, Q., & Sha, Z.-X. (2012). Expression profiles of NODs in channel catfish (Ictalurus punctatus) after infection with Edwardsiella tarda, Aeromonas hydrophila, streptococcus iniae and channel catfish hemorrhage reovirus. Fish & Shellfish Immunology, 33, 1033-1041.
- Li, S.-Y., Xiong, N.-X., Li, K.-X., Huang, J.-F., Ou, J., Wang, F., Huang, M.-Z., & Luo, S.-W. (2024). Cloning, expression and functional characterization of recombinant tumor necrosis factor α1 (TNFα1) from white crucian carp in gut immune regulation. *International Journal* of Biological Macromolecules, 254, 127770.
- Li, Y., Xiao, T., & Zou, J. (2021). Fish TNF and TNF receptors. Science China Life Sciences, 64, 196–220.
- Lian, Z., Bai, J., Hu, X., Lü, A., Sun, J., Guo, Y., & Song, Y. (2020). Detection and characterization of Aeromonas salmonicida subsp. salmonicida infection in crucian carp Carassius auratus. Veterinary Research Communications, 44, 61–72.
- Liu, C. Y., & Kaufman, R. J. (2003). The unfolded protein response. *Journal of Cell Science*, 116, 1861–1862.
- Livak, K. J., & Schmittgen, T. D. (2001). Analysis of relative gene expression data using real-time quantitative PCR and the  $2-\Delta\Delta$ CT method. *Methods*, 25, 402–408.
- Luo, S.-W., Luo, K.-K., & Liu, S.-J. (2020). ITLN in diploid hybrid fish (Carassius auratus cuvieri

  Carassius auratus red var

  is involved in host defense against bacterial infection. *Developmental & Comparative Immunology*, 103, 103520.
- Luo, S.-W., Mao, Z.-W., Luo, Z.-Y., Xiong, N.-X., Luo, K.-K., Liu, S.-J., Yan, T., Ding, Y.-M., Zhao, R.-R., & Wu, C. (2021). Chimeric ferritin H in hybrid crucian carp exhibit a similar down-regulation in lipopolysaccharide-induced NF-κB inflammatory signal in comparison with Carassius cuvieri and Carassius auratus red var. Comparative Biochemistry and Physiology Part C: Toxicology & Pharmacology, 241, 108966.
- Magnadottir, B. (2010). Immunological control of fish diseases. Marine Biotechnology, 12, 361–379.
- Miao, Z., Miao, Z., Teng, X., & Xu, S. (2023). Melatonin alleviates leadinduced fatty liver in the common carps (Cyprinus carpio) via gut-liver axis. Environmental Pollution, 317, 120730.
- Padmini, E., & Usha, R. M. (2011). Heat-shock protein 90 alpha (HSP90α) modulates signaling pathways towards tolerance of oxidative stress and enhanced survival of hepatocytes of Mugil cephalus. *Cell Stress and Chaperones*, 16, 411–425.
- Pelaseyed, T., Bergström, J. H., Gustafsson, J. K., Ermund, A., Birchenough, G. M., Schütte, A., van der Post, S., Svensson, F., Rodríguez-Piñeiro, A. M., & Nyström, E. E. (2014). The mucus and mucins of the goblet cells and enterocytes provide the first defense line of the gastrointestinal tract and interact with the immune system. Immunological Reviews, 260, 8–20.
- Rizwan, S., ReddySekhar, P., & MalikAsrar, B. (2014). Reactive oxygen species in inflammation and tissue injury. Antioxidants & Redox Signaling, 20, 1126–1167.
- Sahreen, A., Fatima, K., Zainab, T., & Saifullah, M. K. (2021). Changes in the level of oxidative stress markers in Indian catfish (Wallago attu) infected with Isoparorchis hypselobagri. Beni-Suef University Journal of Basic and Applied Sciences, 10, 1–8.
- Salinas, I. (2015). The mucosal immune system of teleost fish. *Biology*, 4, 525–539.
- Schneeberger, E. E., & Lynch, R. D. (2004). The tight junction: A multifunctional complex. American Journal of Physiology-Cell Physiology, 286, C1213-C1228.
- Secombes, C., Wang, T., Hong, S., Peddie, S., Crampe, M., Laing, K., Cunningham, C., & Zou, J. (2001). Cytokines and innate immunity of fish. *Developmental & Comparative Immunology*, 25, 713–723.
- Shan, J., Wang, G., Li, H., Zhao, X., Ye, W., Su, L., Zhu, Q., Liu, Y., Cheng, Y., & Zhang, W. (2023). The immunoregulatory role of fish

- specific type II SOCS via inhibiting metaflammation in the gut-liver axis. Water Biology and Security, 2, 100131.
- Tourneur, L., & Chiocchia, G. (2010). FADD: A regulator of life and death. *Trends in Immunology*, 31, 260–269.
- Vanamee, É. S., & Faustman, D. L. (2018). Structural principles of tumor necrosis factor superfamily signaling. *Science Signaling*, 11, eaao4910.
- Wang, F., Qin, Z. L., Luo, W. S., Xiong, N. X., Huang, M. Z., Ou, J., Luo, S. W., & Liu, S. J. (2023). Alteration of synergistic immune response in gut-liver axis of white crucian carp (Carassius cuvieri) after gut infection with Aeromonas hydrophila. *Journal of Fish Diseases*, 00, 1-11.
- Wu, N., Song, Y.-L., Wang, B., Zhang, X.-Y., Zhang, X.-J., Wang, Y.-L., Cheng, Y.-Y., Chen, D.-D., Xia, X.-Q., & Lu, Y.-S. (2016). Fish gutliver immunity during homeostasis or inflammation revealed by integrative transcriptome and proteome studies. *Scientific Reports*, 6.1–17
- Xiong, N.-X., Fang, Z.-X., Kuang, X.-Y., Ou, J., Luo, S.-W., & Liu, S.-J. (2023). Integrated analysis of gene expressions and metabolite features unravel immunometabolic interplay in hybrid fish (Carassius cuvieri

  2 Carassius auratus red var

  3) infected with Aeromonas hydrophila. Aquaculture, 563, 738981.
- Xiong, N.-X., Ou, J., Li, S.-Y., Zhao, J.-H., Huang, J.-F., Li, K.-X., Luo, S.-W., Liu, S.-J., Wen, M., & Wu, C. (2022). A novel ferritin L (FerL) in hybrid crucian carp could participate in host defense against Aeromonas hydrophila infection and diminish inflammatory signals. Fish & Shellfish Immunology, 120, 620–632.

- Xiong, N.-X., Wang, F., Luo, W.-S., Ou, J., Qin, Z.-L., Huang, M.-Z., & Luo, S.-W. (2023). Tumor necrosis factor α2 (TNFα2) facilitates gut barrier breach by Aeromonas hydrophila and exacerbates liver injury in hybrid fish. *Aquaculture*, 577, 739995.
- Yang, C., Yang, S., Miao, Y., Shu, J., Peng, Y., Li, J., Wu, H., Zou, J., & Feng, H. (2023). PRMT6 inhibits K63-linked ubiquitination and promotes the degradation of IRF3 in the antiviral innate immunity of black carp Mylopharyngodon piceus. Aquaculture, 562, 738872.
- Yenari, M. A., Liu, J., Zheng, Z., Vexler, Z. S., Lee, J. E., & Giffard, R. G. (2005). Antiapoptotic and anti-inflammatory mechanisms of heatshock protein protection. *Annals of the new York Academy of Sciences*, 1053, 74–83.
- Zhang, J., Wang, J.-Q., Xu, X.-Y., Yang, J.-Y., Wang, Z., Jiang, S., Wang, Y.-P., Zhang, J., Zhang, R., & Li, W. (2020). Red ginseng protects against cisplatin-induced intestinal toxicity by inhibiting apoptosis and autophagy via the PI3K/AKT and MAPK signaling pathways. *Food & Function*, 11, 4236–4248.

#### SUPPORTING INFORMATION

Additional supporting information can be found online in the Supporting Information section at the end of this article.

How to cite this article: Li, K.-X., Xiong, N.-X., Huang, J.-F., Li, S.-Y., Ou, J., Wang, F., & Luo, S.-W. (2024). Tumor necrosis factor  $\alpha 1$  decreases mucosal immune and antioxidant response in the midgut of hybrid fish (white crucian carp  $\varphi \times \text{red crucian carp } \vartheta$ ). *Journal of Fish Biology*, 1–11. <a href="https://doi.org/10.1111/jfb.15733">https://doi.org/10.1111/jfb.15733</a>